Reactions of Co-ordinated Ligands. Part 31.[1] The Synthesis, Structure, and Protonation of the Octamethyloctatrienediylidenedimolybdenum Complex $[Mo_2(\mu\text{-}C_8Me_8)(\eta\text{-}C_5H_5)_2]$,† Evidence for Three-centre Carbon–Hydrogen–Molybdenum Interactions

Michael Green,* Nicholas C. Norman, A. Guy Orpen, and Colin J. Schaverien
Department of Inorganic Chemistry, The University, Bristol BS8 1TS

Reaction of $[Mo(NCMe)(MeC_2Me)_2(\eta\text{-}C_5H_5)][BF_4]$ with $Na[Fe(CO)_2(\eta^5\text{-}C_5H_5)]$ in tetrahydrofuran affords $[Fe_2(CO)_4(\eta\text{-}C_5H_5)_2]$ and the octamethyloctatrienediylidenedimolybdenum complex $[Mo_2(\mu\text{-}C_8Me_8)(\eta\text{-}C_5H_5)_2]$ (1) identified by *X*-ray diffraction studies. Complex (1) crystallizes in the triclinic space group $P\bar{1}$, with a = 8.449(1), b = 10.114(2), c = 14.872(3) Å, α = 86.66(2), β = 80.88(1), γ = 63.78(1), and Z = 2. The structure was refined to R = 0.020 and R' = 0.025. The molecular structure of complex (1) shows non-crystallographic C_s symmetry, and there is a formal Mo=Mo double bond [Mo=Mo 2.595(1) Å]. The C_8 carbon chain binds to the dimolybdenum unit in an σ, η^3, η^2, η^3, σ fashion such that it forms σ bonds to one molybdenum atom of mean length 2.092(2) Å, each molybdenum atom carrying an η^5-cyclopentadienyl group. Extended-Hückel molecular orbital calculations on complex (1) indicate an accumulation of electron density on the carbon atoms of the C_8 chain, and in agreement with this finding protonation with $HBF_4{\cdot}OEt_2$ or CF_3CO_2H affords purple crystals of $[Mo_2(\mu\text{-}C_8Me_8)(\mu_{Mo,C}\text{-}H)(\eta\text{-}C_5H_5)_2]BF_4$ (2) and $[Mo_2(\mu\text{-}C_8Me_8)(\mu_{Mo,C}\text{-}H)(\eta\text{-}C_5H_5)_2][(CF_3CO_2)_2H]$ (3). The ^1H n.m.r. spectra of these cations showed a high-field signal due to the proton derived from the acid indicating the presence of a CHMo system. This was confirmed by an *X*-ray crystallographic study on complex (3), which crystallizes in the monoclinic space group $P2_1/c$, with a = 10.648(2), b = 15.119(4), c = 19.655(6) Å, β = 105.30(2)°, and Z = 4; the structure was refined to R = 0.029 and R' = 0.034. The crystal structure of complex (3) contains isolated $[Mo_2(\mu\text{-}C_8Me_8)(\mu_{Mo,C}\text{-}H)(\eta\text{-}C_5H_5)_2]^+$ cations and $[(CF_3CO_2)_2H]^-$ anions. The cation non-hydrogen atom geometry is closely similar to that of complex (1), with the exception that one of the terminal Mo–C σ bonds is markedly extended [to 2.196(5) Å]. This bond is bridged by a hydrogen atom which shows Mo–H and C–H distances of 1.88(8) and 0.89(8) Å, and an Mo–H–C angle 99(5)°. The complex anion contains two CF_3CO_2 units linked by a strong, short hydrogen bond [O · · · O 2.429(8), O(311)–H(42) 1.35(7), and O(412)–H(42) 1.08(7) Å]. Examination of the variable-temperature (192—295 K) ^{13}C n.m.r. spectra of the cation $[Mo_2(\mu\text{-}C_8Me_8)(\mu_{Mo,C}\text{-}H)(\eta\text{-}C_5H_5)_2]^+$ suggests that in solution the bridging proton undergoes site exchange such that it spends some time attached to the terminal carbon atom (C_α) of the C_8 chain, and the remainder attached to one of the olefinic carbon atoms (C_δ), in both cases bridging from these to the molybdenum atom.

The chemistry of complexes in which carbon to hydrogen bonds interact with transition-metal centres has been an area of great interest in recent years.[2,3,4] Such species are involved in the scission and formation of C–H bonds by transition metals, and theoretical, structural, and spectroscopic investigations of species containing C–H–M systems have been reported leading to a growth of understanding of these important interactions. It is possible that these insights may ultimately lead to the development of homogeneous transition-metal catalysts capable of functionalizing aliphatic hydrocarbons.

A range of three-centre interactions have been identified, in which the C–H–M array varies in geometry from a linear arrangement to a 'closed' geometry. In exploring the reactions of octatrienediylidenedimolybdenum complexes we observed [5] that protonation of $[Mo_2(\mu\text{-}C_8Me_8)(\eta\text{-}C_5H_5)_2]$ afforded the cation $[Mo_2(\mu\text{-}C_8Me_8)(\mu_{Mo,C}\text{-}H)(\eta\text{-}C_5H_5)_2]^+$, in which electron deficiency at a molybdenum centre is reduced by interaction with an adjacent C–H bond. This paper reports a detailed study of this chemistry.

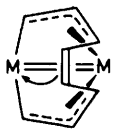

(I)

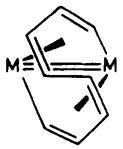

(II)

Results and Discussion

Dimolybdenum species containing two, three, and four linked alkyne molecules have been synthesized by reaction (refluxing octane) of $[Mo_2(CO)_4(\eta\text{-}C_5H_5)_2]$ with the respective alkyne.[6,7] In the case of alkynes carrying electronegative substituents two structural forms (I) and (II) of alkyne tetramers complexed to dimetal centres have been identified. One involves a molybdenacyclononatetraene moiety to which is bonded the second metal, the C_8 chain beginning and ending with σ bonds to the same metal atom. The second form also has an unbranched C_8 chain, but this begins and ends with σ bonds to different metal atoms, and therefore, may be des-

† μ-[η-3,4,5,6,7,8-Hexamethyldeca-3,5,7-triene-2,9-diylidene-$C^{2,5-6,9}(Mo^1)C^{2-4,7-9}(Mo^2)$]-bis(η-cyclopentadienylmolybdenum) (*Mo=Mo*) and its cationic analogue μ-[η-3,4,5,6,7,8-hexamethyldeca-3,5,7-trien-2-yl-9-ylidene-$C^{2,5-6,9}(Mo^1)C^{2-4,7-9}(Mo^2)$]-bis(η-cyclopentadienylmolybdenum)(*Mo=Mo*)(1+) bis(trifluoroacetato)-hydrogenate.

Supplementary data available (No. SUP 23971, 53 pp.): thermal parameters, structure factors. See Instructions for Authors, *J. Chem. Soc., Dalton Trans.*, 1984, Issue 1, pp. xvii—xix.

Non-S.I. unit employed: eV ≈ 1.60 × 10^{-19} J.

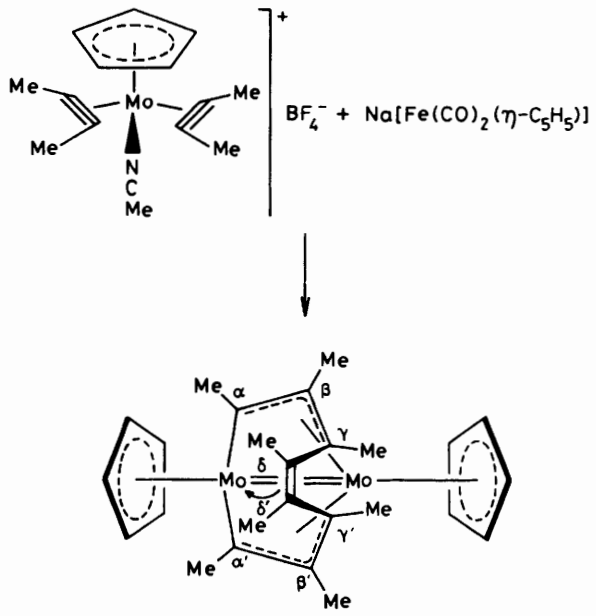

(1)

cribed as a C_8 'flyover' or a dimetallacyclodecapentaene.* Both these unsaturated systems are potentially electron rich and might be expected to react with electrophilic reagents. An opportunity to examine the protonation of a molybdenacyclononatetraene–molybdenum complex was provided by our discovery of a simple synthetic pathway to $[Mo_2(\mu\text{-}C_8Me_8)(\eta\text{-}C_5H_5)_2]$.

Treatment of $[Mo(NCMe)(MeC_2Me)_2(\eta\text{-}C_5H_5)]^+$, as its BF_4^- salt, with sodium dicarbonylcyclopentadienylferrate in tetrahydrofuran affords † $[Fe_2(CO)_4(\eta\text{-}C_5H_5)_2]$, and the purple crystalline complex $[Mo_2(\mu\text{-}C_8Me_8)(\eta\text{-}C_5H_5)_2]$ (1). The complex (1) was characterized by ^1H and ^{13}C n.m.r., mass spectrometry, and elemental analysis. The n.m.r. spectra (see Table 1) show the molecule to possess time-averaged C_s symmetry in solution, and thus belong to the first class of M_2C_8 complexes as described above. The dimolybdenum and ditungsten species $[M_2\{\mu\text{-}C_8(CO_2Me)_8\}(\eta\text{-}C_5H_5)_2]$ (M = Mo or W) prepared by Stone and co-workers [6] have structures analogous to that of complex (1). Despite the very different electronegativity of the substituents in these complexes as compared with (1) they show ^{13}C resonances for the carbon atoms of the C_8 chain which are very similar in pattern to those of complex (1). The main contrast in n.m.r. parameters involves the ^1H resonances for the cyclopentadienyl protons, which show a more marked differentation between the two groups in complex (1) than in the methoxycarbonyl substituted complexes {chemical shift difference <0.06 p.p.m. for $[M_2\{\mu\text{-}C_8(CO_2Me)_8\}(\eta\text{-}C_5H_5)_2]$, *cf.* 1.29 p.p.m. for (1)}.

In order to characterize structurally the effect of changing the electronegativity of the substituents, R, in the $[Mo_2(\mu\text{-}C_8R_8)(\eta\text{-}C_5H_5)_2]$ system, and to provide a basis for discussion

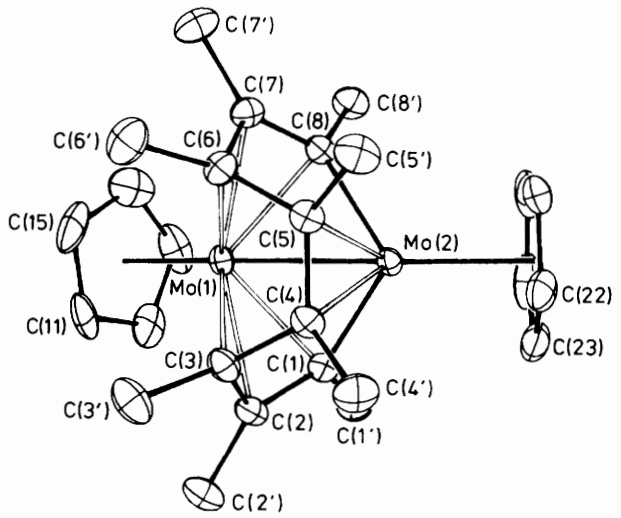

Figure 1. Molecular geometry of $[Mo_2(\mu\text{-}C_8Me_8)(\eta\text{-}C_5H_5)_2]$ (1)

of the geometry of derivatives of complex (1), it was subjected to an *X*-ray diffraction study. The derived bond lengths and interbond angles within the molecule are given in Tables 2 and 3. The molecular geometry of complex (1) is illustrated in Figure 1, in which only the major orientation of the disordered cyclopentadienyl ligand bonded to Mo(1) is shown. The crystal structure of complex (1) consists of discrete molecules separated by normal van der Waals distances. The $Mo_2(\mu\text{-}C_8Me_8)$ core of the molecule shows non-crystallographic C_s symmetry within experimental uncertainty. The connectivity of the C_8 chain is similar to that observed [7] in $[Mo_2\{\mu\text{-}C_8(CO_2Me)_6H_2\}(\eta\text{-}C_5H_5)_2]$. This involves C_8 chain co-ordination in a σ, η^3, η^2, η^3, σ, or μ-allylidene, olefin, μ-allylidene fashion. The μ-allylidene fragment has been observed in a number of homo- and hetero-dinuclear species, for example, $[Ru_2\{\mu\text{-}C(Me)C(Me)C(Me)CH_2\}(CO)_2(\eta\text{-}C_5H_5)_2]$,[10] $[Fe_2\{\mu\text{-}C(CO_2Me)C(CO_2Me)CHMe\}(CO)_2(\eta\text{-}C_5H_5)_2]$,[11] $[Mo_2(\mu\text{-}CHCHCMe_2)(CO)_4(\eta\text{-}C_5H_5)_2]$,[12] and $[(\eta\text{-}C_5H_5)Co\{\mu\text{-}C(C_6H_4Me\text{-}p)C(Me)CHMe\}W(CO)_2(\eta\text{-}C_5H_5)]$.[13] In all these systems the allylidene moiety can be considered to act as a neutral four-electron donor. Characteristic of these species is a low-field ^{13}C resonance due to the bridging carbon atom of the allylidene moiety [at δ 175.6, 173.4, 174.9, and 192.3 p.p.m. respectively for the four complexes above, *cf.* δ 174.3 p.p.m. for C_α in (1)]. The Mo–Mo bond order in complex (1) is predicted by the effective atomic number rule to be two. The Mo(1)–Mo(2) distance in complex (1) is 2.595(1) Å, slightly shorter than in $[Mo_2\{\mu\text{-}C_8(CO_2Me)_6H_2\}(\eta\text{-}C_5H_5)_2]$ [2.618(1) Å],[6] but in the range observed for other Mo=Mo bonds which are formally double, *e.g.* $[Mo_2(\mu\text{-}C_2Ph_2)(\mu\text{-}C_5Ph_4O)(CO)_3(\eta^4\text{-}C_4Ph_4)]$,[14] Mo=Mo 2.772(4) Å, $[Mo_2(\mu\text{-}SBu^t)_2(CO)_2(\eta\text{-}C_5H_5)_2]$,[15] Mo=Mo 2.616(2) Å, $[Mo_2(OPr^i)_8]$,[16] Mo=Mo 2.523 Å, and $[Mo_2(\mu\text{-}CO)(\mu\text{-}OBu^t)_2(OBu^t)_2]$,[17] Mo=Mo 2.498(1) Å.

The Mo–C bond lengths show the strength of the terminal Mo(2)–C(1) and Mo(2)–C(8) bonds [mean 2.092(2) Å] as compared with the other Mo(1)–C and Mo(2)–C bonds, which are longer [averaged Mo(1)–C_α 2.237(2), Mo(1)–C_β 2.348(2), Mo(1)–C_γ 2.315(2), and Mo(2)–C_δ 2.234(2) Å]. These latter interactions involve ligand donor orbitals of the π type, the terminal Mo(2)–C_α interaction involving a ligand donor orbital of σ symmetry. The C–C bond lengths within the C_8 chain show a similar pattern to those of $[Mo_2\{\mu\text{-}C_8(CO_2Me)_6H_2\}(\eta\text{-}C_5H_5)_2]$. The precision of this study shows the C_γ–C_δ bond to be significantly longer than C_α–C_β, C_β–C_γ,

* Reaction of $[Cr(\eta\text{-}C_5H_5)_2]$ with $Na_2(C_8H_8)$ has been shown to lead to carbon–carbon bond cleavage and the formation of the C_8 'flyover' complex $[Cr_2(\mu\text{-}C_8H_8)(\eta\text{-}C_5H_5)_2]$.[8]

† This apparent redox reaction poses a mechanistic problem in that the termini of the chain formed from four alkyne molecules finally end up linked to just one molybdenum centre. However, we defer discussions of the possible reaction pathways to complex (1) for a paper in preparation on the related reactions with unsymmetrical alkynes and indenyl complexes.[9]

Table 1. N.m.r. spectroscopic data for compounds (1)—(5) at 295 K

Compound	^1H (δ)	^{13}C-{^1H} (δ)
(1) [a,b]	5.09 (s, 5 H, C_5H_5), 3.80 (s, 5 H, C_5H_5), 2.40 (s, 6 H, 2 Me), 2.25 (s, 6 H, 2 Me), 2.00 (s, 6 H, 2 Me), and 0.99 (s, 6 H, 2 Me)	174.3 (2 C), 119.6 (2 C), 97.4 (C_5H_5), 91.3 (C_5H_5), 71.0 (2 C), 69.0 (2 C), 33.0 (2 Me), 25.2 (2 Me), 22.0 (2 Me), and 18.4 (2 Me)
(2) [c,d]	5.48 (s, 5 H, C_5H_5), 4.59 (s, 5 H, C_5H_5), 2.69 (s, 3 H, Me), 2.67 (s, 3 H, Me), 2.66 (s, 3 H, Me), 2.48 [d, 3 H, Me, ^3J(HH) 2.4 Hz], 2.11 (s, 3 H, Me), 2.01 (s, 3 H, Me), 0.95 [d, 3 H, Me, ^3J(HH) 1.4 Hz], 0.93 (s, 3 H, Me), and −9.33 (br m, 1 H, CHMo)	192.5, 144.5, 128.2, 121.4, 83.1, 81.6 (2 C), and 64.4 (C_8 ring); 99.5 (C_5H_5), 97.4 (C_5H_5), 35.2 (Me), 31.1 (Me), 30.9 (Me), 26.1 (Me), 21.9 (Me), 21.7, (Me), 21.6 (Me), and 19.2 (Me)
(5) [c]	5.48 (s, 5 H, C_5H_5), 4.63 (s, 5 H, C_5H_5), 2.75 (s, 3 H, Me), 2.70 (s, 3 H, Me), 2.69 (s, 3 H, Me), 2.58 [d, 3 H, Me, ^3J(HH) 1.46 Hz], 2.28 [ddq, 1 H, CH_2, ^2J(HH) 14.8, ^3J(HH) 7.6, ^3J(HH) 1.6 Hz], 2.16 [ddq, 1 H, CH_2, ^2J(HH) 14.9, ^3J(HH) 7.6, ^3J(HH) 2.8 Hz], 1.99 (s, 3 H, Me), 1.90 (s, 3 H, Me), 0.83 [t, 3 H, Me, ^3J(HH) 7.6 Hz], 0.72 [t, 3 H, Me, ^3J(HH) 7.6 Hz], 0.13 [ddq, 1 H, CH_2, ^3J(HH) 1.71, ^2J(HH) 14.8, ^3J(HH) 7.3 Hz], −0.076 [dq, 1 H, CH_2, ^2J(HH) 14.8, ^3J(HH) 7.3], and −9.72 (br m, CHMo)	191.1, 160.78, 129.4, 122.4, 88.1, 79.3, 77.0, and 61.8 (C_8 ring); 99.6 (C_5H_5), 97.7 (C_5H_5), 35.0, 32.4, 29.6, 25.6, 21.3, 20.9, 20.2, 18.2, 12.1, and 12.0 (8 Me + 2 CH_2)

[a] Measured in C_6D_6. [b] ^{95}Mo N.m.r. (C_6D_6): δ 579 and −221 p.p.m. Positive values to high frequency, reference Na_2MoO_4 (2 mol dm^{-3}) in NaOH. The linewidths at half-height are 250 and 150 Hz, respectively. The spectrum was recorded on a Bruker WH-400 Fourier-transform spectrometer. [c] Measured in CD_2Cl_2. [d] The data for complex (3) are identical to data for (2) apart from the appearance in the ^1H spectrum of an additional broad singlet at δ 13.5 p.p.m. [1 H, $(CF_3CO_2)_2H$]. The data for complex (4) are identical to data for (3) except the ^1H signals at δ 13.5 and −9.33 p.p.m. are absent, and the two Me resonances coupled to the high-field proton appear as singlets.

Table 2. Bond lengths (Å) for $[Mo_2(\mu\text{-}C_8Me_8)(\eta\text{-}C_5H_5)_2]$ (1) *

Mo(1)–Mo(2)	2.595(1)	Mo(1)–C(11′)	2.397(11)	Mo(2)–C(24)	2.377(4)	C(6)–C(5)	1.507(3)
Mo(1)–C(1)	2.238(2)	Mo(1)–C(12′)	2.317(9)	Mo(2)–C(25)	2.368(4)	C(6)–C(7)	1.434(4)
Mo(1)–C(2)	2.346(2)	Mo(1)–C(13′)	2.274(10)	C(1)–C(2)	1.418(4)	C(6)–C(6′)	1.522(4)
Mo(1)–C(3)	2.312(3)	Mo(1)–C(14′)	2.330(11)	C(1)–C(1′)	1.525(3)	C(7)–C(8)	1.416(3)
Mo(1)–C(6)	2.318(2)	Mo(1)–C(15′)	2.405(11)	C(2)–C(3)	1.428(3)	C(7)–C(7′)	1.517(3)
Mo(1)–C(7)	2.349(2)	Mo(2)–C(1)	2.088(2)	C(2)–C(2′)	1.525(4)	C(8)–C(8′)	1.528(4)
Mo(1)–C(8)	2.236(2)	Mo(2)–C(4)	2.235(3)	C(3)–C(4)	1.507(3)	C(21)–C(22)	1.395(4)
Mo(1)–C(11)	2.391(3)	Mo(2)–C(5)	2.232(2)	C(3)–C(3′)	1.531(5)	C(21)–C(25)	1.405(5)
Mo(1)–C(12)	2.363(3)	Mo(2)–C(8)	2.095(2)	C(4)–C(5)	1.442(3)	C(22)–C(23)	1.393(3)
Mo(1)–C(13)	2.331(3)	Mo(2)–C(21)	2.409(2)	C(4)–C(4′)	1.529(3)	C(23)–C(24)	1.396(5)
Mo(1)–C(14)	2.339(4)	Mo(2)–C(22)	2.422(2)	C(5)–C(5′)	1.531(3)	C(24)–C(25)	1.400(5)
Mo(1)–C(15)	2.376(3)	Mo(2)–C(23)	2.420(3)				

* Estimated standard deviations in the least significant digit are in parentheses here and throughout this paper. C(11′)—C(15′) are the atoms of the disordered cyclopentadienyl group of lower occupancy.

Table 3. Bond angles (°) for $[Mo_2(\mu\text{-}C_8Me_8)(\eta\text{-}C_5H_5)_2]$ (1)

Mo(2)–Mo(1)–C(1)	50.5(1)	C(7)–Mo(1)–C(8)	35.9(1)	Mo(1)–C(2)–C(2′)	129.3(1)	C(6)–C(5)–C(5′)	114.5(2)
Mo(2)–Mo(1)–C(2)	74.3(1)	Mo(1)–Mo(2)–C(1)	55.8(1)	C(1)–C(2)–C(2′)	124.4(2)	Mo(1)–C(6)–C(5)	97.1(1)
C(1)–Mo(1)–C(2)	35.9(1)	Mo(1)–Mo(2)–C(4)	73.8(1)	C(3)–C(2)–C(2′)	122.3(3)	Mo(1)–C(6)–C(7)	73.3(1)
Mo(2)–Mo(1)–C(3)	73.7(1)	C(1)–Mo(2)–C(4)	78.6(1)	Mo(1)–C(3)–C(2)	73.4(1)	C(5)–C(6)–C(7)	114.3(2)
C(1)–Mo(1)–C(3)	62.9(1)	Mo(1)–Mo(2)–C(5)	73.9(1)	Mo(1)–C(3)–C(4)	97.3(2)	Mo(1)–C(6)–C(6′)	125.0(2)
C(2)–Mo(1)–C(3)	35.7(1)	C(1)–Mo(2)–C(5)	108.3(1)	C(2)–C(3)–C(4)	114.3(2)	C(5)–C(6)–C(6′)	117.4(2)
Mo(2)–Mo(1)–C(6)	73.7(1)	C(4)–Mo(2)–C(5)	37.7(1)	Mo(1)–C(3)–C(3′)	125.0(2)	C(7)–C(6)–C(6′)	120.5(2)
C(1)–Mo(1)–C(6)	115.3(1)	Mo(1)–Mo(2)–C(8)	55.7(1)	C(2)–C(3)–C(3′)	120.3(2)	Mo(1)–C(7)–C(6)	70.9(1)
C(2)–Mo(1)–C(6)	107.5(1)	C(1)–Mo(2)–C(8)	104.8(1)	C(4)–C(3)–C(3′)	117.4(2)	Mo(1)–C(7)–C(8)	67.7(1)
C(3)–Mo(1)–C(6)	73.3(1)	C(4)–Mo(2)–C(8)	108.2(1)	Mo(2)–C(4)–C(3)	102.4(1)	C(6)–C(7)–C(8)	113.3(2)
Mo(2)–Mo(1)–C(7)	74.3(1)	C(5)–Mo(2)–C(8)	78.6(1)	Mo(2)–C(4)–C(5)	71.1(1)	Mo(1)–C(7)–C(7′)	129.8(1)
C(1)–Mo(1)–C(7)	124.8(1)	Mo(1)–C(1)–Mo(2)	73.6(1)	C(3)–C(4)–C(5)	116.1(2)	C(6)–C(7)–C(7′)	122.5(2)
C(2)–Mo(1)–C(7)	137.8(1)	Mo(1)–C(1)–C(2)	76.2(1)	Mo(2)–C(4)–C(4′)	122.7(2)	C(8)–C(7)–C(7′)	124.3(3)
C(3)–Mo(1)–C(7)	107.6(1)	Mo(1)–C(1)–C(1′)	126.9(1)	C(3)–C(4)–C(4′)	113.6(2)	Mo(1)–C(8)–Mo(2)	73.5(1)
C(6)–Mo(1)–C(7)	35.8(1)	Mo(2)–C(1)–C(2)	115.7(1)	C(5)–C(4)–C(4′)	122.8(2)	Mo(1)–C(8)–C(7)	76.4(1)
Mo(2)–Mo(1)–C(8)	50.7(1)	Mo(2)–C(1)–C(1′)	123.3(2)	Mo(2)–C(5)–C(4)	71.3(1)	Mo(2)–C(8)–C(7)	115.7(2)
C(1)–Mo(1)–C(8)	95.6(1)	C(2)–C(1)–C(1′)	120.4(2)	Mo(2)–C(5)–C(6)	102.6(1)	Mo(1)–C(8)–C(8′)	126.6(1)
C(2)–Mo(1)–C(8)	125.0(1)	Mo(1)–C(2)–C(1)	67.9(1)	C(4)–C(5)–C(6)	116.0(2)	Mo(2)–C(8)–C(8′)	123.8(2)
C(3)–Mo(1)–C(8)	115.6(1)	Mo(1)–C(2)–C(3)	70.9(1)	Mo(2)–C(5)–C(5′)	121.2(2)	C(7)–C(8)–C(8′)	120.0(2)
C(6)–Mo(1)–C(8)	63.0(1)	C(1)–C(2)–C(3)	113.3(2)	C(4)–C(5)–C(5′)	122.6(2)		

Table 4. Bond lengths (Å) for $[Mo_2(\mu\text{-}C_8Me_8)(\mu_{Mo,C}\text{-}H)(\eta\text{-}C_5H_5)_2][(CF_3CO_2)_2H]$ (3)

Mo(1)–Mo(2)	2.614(1)	Mo(2)–C(21)	2.376(5)	C(6)–C(6′)	1.527(7)	C(31)–O(311)	1.234(7)
Mo(1)–C(1)	2.216(5)	Mo(2)–C(22)	2.360(5)	C(7)–C(8)	1.436(7)	C(31)–O(312)	1.207(7)
Mo(1)–C(2)	2.350(4)	Mo(2)–C(23)	2.345(5)	C(7)–C(7′)	1.520(9)	C(32)–F(321)	1.310(7)
Mo(1)–C(3)	2.318(4)	Mo(2)–C(24)	2.361(4)	C(8)–C(8′)	1.518(6)	C(32)–F(322)	1.300(9)
Mo(1)–C(6)	2.341(5)	Mo(2)–C(25)	2.374(6)	C(21)–C(22)	1.387(7)	C(32)–F(323)	1.259(7)
Mo(1)–C(7)	2.321(4)	C(1)–C(2)	1.426(5)	C(21)–C(25)	1.384(9)	C(41)–C(42)	1.509(9)
Mo(1)–C(8)	2.234(4)	C(1)–C(1′)	1.525(7)	C(22)–C(23)	1.385(8)	C(41)–O(411)	1.192(6)
Mo(1)–C(11)	2.320(4)	C(2)–C(3)	1.414(6)	C(23)–C(24)	1.408(9)	C(41)–O(412)	1.232(8)
Mo(1)–C(12)	2.342(5)	C(2)–C(2′)	1.504(6)	C(24)–C(25)	1.391(10)	C(42)–F(421)	1.321(9)
Mo(1)–C(13)	2.369(5)	C(3)–C(4)	1.499(5)	C(11)–C(12)	1.389(7)	C(42)–F(422)	1.287(8)
Mo(1)–C(14)	2.370(6)	C(3)–C(3′)	1.519(6)	C(11)–C(15)	1.397(8)	C(42)–F(423)	1.248(10)
Mo(1)–C(15)	2.339(5)	C(4)–C(5)	1.429(7)	C(12)–C(13)	1.400(7)	Mo(2)–H(8)	1.88(8)
Mo(2)–C(1)	2.130(4)	C(4)–C(4′)	1.530(7)	C(13)–C(14)	1.388(8)	C(8)–H(8)	0.89(8)
Mo(2)–C(4)	2.241(4)	C(5)–C(5′)	1.540(7)	C(14)–C(15)	1.393(7)	O(311)–H(42)	1.35(7)
Mo(2)–C(5)	2.287(4)	C(6)–C(5)	1.524(7)	C(31)–C(32)	1.508(8)	O(412)–H(42)	1.08(7)
Mo(2)–C(8)	2.196(5)	C(6)–C(7)	1.412(6)				

Table 5. Bond angles (°) for $[Mo_2(\mu\text{-}C_8Me_8)(\mu_{Mo,C}\text{-}H)(\eta\text{-}C_5H_5)_2][(CF_3CO_2)_2H]$ (3)

H(8)–Mo(2)–Mo(1)	72(3)	C(1)–Mo(1)–C(3)	63.0(1)	C(3)–C(2)–C(2′)	122.4(4)	Mo(1)–C(7)–C(7′)	127.7(3)
H(8)–Mo(2)–C(1)	125(3)	C(2)–Mo(1)–C(3)	35.2(1)	Mo(1)–C(3)–C(2)	73.6(2)	C(6)–C(7)–C(7′)	122.6(5)
H(8)–Mo(2)–C(4)	100(3)	Mo(2)–Mo(1)–C(6)	74.4(1)	Mo(1)–C(3)–C(4)	97.4(2)	C(8)–C(7)–C(7′)	122.0(4)
H(8)–Mo(2)–C(5)	65(3)	C(1)–Mo(1)–C(6)	115.8(2)	C(2)–C(3)–C(4)	114.6(4)	Mo(1)–C(8)–Mo(2)	72.3(1)
H(8)–Mo(2)–C(8)	24(3)	C(2)–Mo(1)–C(6)	105.7(2)	Mo(1)–C(3)–C(3′)	125.1(3)	Mo(1)–C(8)–C(7)	75.0(2)
H(8)–Mo(2)–C(21)	132(2)	C(3)–Mo(1)–C(6)	71.5(2)	C(2)–C(3)–C(3′)	120.0(4)	Mo(2)–C(8)–C(7)	113.3(3)
H(8)–Mo(2)–C(22)	136(3)	Mo(2)–Mo(1)–C(7)	76.4(1)	C(4)–C(3)–C(3′)	117.1(4)	Mo(1)–C(8)–C(8′)	126.2(3)
H(8)–Mo(2)–C(23)	102(3)	C(1)–Mo(1)–C(7)	128.0(2)	Mo(2)–C(4)–C(3)	103.3(2)	Mo(2)–C(8)–C(8′)	124.2(3)
H(8)–Mo(2)–C(24)	81(3)	C(2)–Mo(1)–C(7)	137.2(2)	Mo(2)–C(4)–C(5)	73.4(2)	C(7)–C(8)–C(8′)	122.2(4)
H(8)–Mo(2)–C(25)	98(3)	C(3)–Mo(1)–C(7)	105.9(2)	C(3)–C(4)–C(5)	116.1(4)	C(32)–C(31)–O(311)	112.8(5)
H(8)–C(8)–Mo(1)	112(5)	C(6)–Mo(1)–C(7)	35.3(2)	Mo(2)–C(4)–C(4′)	121.0(3)	C(32)–C(31)–O(312)	117.8(5)
H(8)–C(8)–Mo(2)	58(6)	Mo(2)–Mo(1)–C(8)	53.2(1)	C(3)–C(4)–C(4′)	113.5(4)	O(311)–C(31)–O(312)	129.4(5)
H(8)–C(8)–C(7)	85(6)	C(1)–Mo(1)–C(8)	99.4(2)	C(5)–C(4)–C(4′)	122.3(4)	C(31)–C(32)–F(321)	111.1(5)
H(8)–C(8)–C(8′)	119(5)	C(2)–Mo(1)–C(8)	128.1(2)	Mo(2)–C(5)–C(4)	69.8(2)	C(31)–C(32)–F(322)	114.2(5)
Mo(1)–Mo(2)–C(1)	54.5(1)	C(3)–Mo(1)–C(8)	116.5(1)	Mo(2)–C(5)–C(6)	102.1(3)	F(321)–C(32)–F(322)	101.6(6)
Mo(1)–Mo(2)–C(4)	73.4(1)	C(6)–Mo(1)–C(8)	63.4(1)	C(4)–C(5)–C(6)	114.6(3)	C(31)–C(32)–F(323)	116.0(6)
C(1)–Mo(2)–C(4)	77.6(1)	C(7)–Mo(1)–C(8)	36.7(2)	Mo(2)–C(5)–C(5′)	127.3(3)	F(321)–C(32)–F(323)	107.0(6)
Mo(1)–Mo(2)–C(5)	73.9(1)	Mo(1)–C(1)–Mo(1)	73.9(1)	C(4)–C(5)–C(5′)	121.4(4)	F(322)–C(32)–F(323)	105.6(6)
C(1)–Mo(2)–C(5)	106.6(1)	Mo(1)–C(1)–C(2)	77.0(3)	C(6)–C(5)–C(5′)	114.0(5)	C(42)–C(41)–O(411)	119.9(6)
C(4)–Mo(2)–C(5)	36.8(2)	Mo(2)–C(1)–C(2)	115.2(3)	Mo(1)–C(6)–C(5)	97.6(3)	C(42)–C(41)–O(412)	110.8(5)
Mo(1)–Mo(2)–C(8)	54.5(1)	Mo(1)–C(1)–C(1′)	126.1(3)	Mo(1)–C(6)–C(7)	71.6(3)	O(411)–C(41)–O(412)	129.2(6)
C(1)–Mo(2)–C(8)	103.3(2)	Mo(2)–C(1)–C(1′)	123.7(3)	C(5)–C(6)–C(7)	116.6(4)	C(41)–C(42)–F(421)	111.5(5)
C(4)–Mo(2)–C(8)	106.3(2)	C(2)–C(1)–C(1′)	120.4(3)	Mo(1)–C(6)–C(6′)	125.5(3)	C(41)–C(42)–F(422)	114.7(6)
C(5)–Mo(2)–C(8)	77.9(2)	Mo(1)–C(2)–C(1)	66.7(2)	C(5)–C(6)–C(6′)	116.7(4)	F(421)–C(42)–F(422)	100.5(6)
Mo(2)–Mo(1)–C(1)	51.5(1)	Mo(1)–C(2)–C(3)	71.1(2)	C(7)–C(6)–C(6′)	119.7(5)	C(41)–C(42)–F(423)	113.3(6)
Mo(2)–Mo(1)–C(2)	74.9(1)	C(1)–C(2)–C(3)	113.2(3)	Mo(1)–C(7)–C(6)	73.1(3)	F(421)–C(42)–F(423)	107.2(7)
C(1)–Mo(1)–C(2)	36.2(1)	Mo(1)–C(2)–C(2′)	129.9(3)	Mo(1)–C(7)–C(8)	68.4(2)	F(422)–C(42)–F(423)	108.8(5)
Mo(2)–Mo(1)–C(3)	73.7(1)	C(1)–C(2)–C(2′)	124.4(4)	C(6)–C(7)–C(8)	115.3(4)		

or C_δ–$C_{\delta'}$ [average 1.507(3) *vs.* 1.417(4), 1.431(4), and 1.442(3) Å respectively]. In addition the C–C–C–C intrachain torsion angles show the C_γ–C_δ bond to be close to single [mean C_α–C_β–C_γ–C_δ 36.3(2), C_β–C_γ–C_δ–$C_{\delta'}$ 117.9(2), and C_γ–C_δ–$C_{\delta'}$–$C_{\gamma'}$ 0.4(3)°]. This is in accord with the description given above of the bonding of the μ-C_8Me_8 moiety. Apparently the electronegativity of the chain substituents has remarkably little effect on the structure of the $Mo_2(\mu\text{-}C_8)$ core of these $[Mo_2(\mu\text{-}C_8R_8)(\eta\text{-}C_5H_5)_2]$ molecules.

Extended-Hückel molecular-orbital (EHMO) calculations [18] were performed on $[Mo_2(\mu\text{-}C_8H_8)(\eta\text{-}C_5H_5)_2]$ using the geometry derived from the crystallographic results on complex (1), C–H lengths set to 1.08 Å, and parameters taken from the literature.[18] These showed a number of interesting features, which are germane to the observed chemistry of complex (1). In particular these calculations show a fairly small highest occupied molecular orbital–lowest unoccupied molecular orbital (h.o.m.o.–l.u.m.o.) gap of 1.0 eV, the h.o.m.o. being largely metal–metal σ^* in character, and the l.u.m.o. primarily located on Mo(2). The net atomic overlap between Mo(1) and Mo(2) is relatively large (0.309). These features are in accord with the formal unsaturation and Mo=Mo double bond order in complex (1). Most importantly the sites of electron-density accumulation in the molecule are clearly indicated to be the α carbon atoms. These show net charges of −0.54 e [*cf.* Mo(1), +1.32; Mo(2), +0.96; C_β, 0.000; C_γ, −0.21; C_δ, −0.21; and C(of C_5H_5), *ca.* 0.08 e].† Charge build-up on bridging carbene-carbon atoms in dinuclear metal systems has been previously noted in theoretical and u.v. photoelectron spectroscopic (p.e.s.) studies,[19] although the evidence from *X*-ray diffraction is equivocal.[20] Its appearance in complex (1) is, therefore, not unexpected in view of the carbenoid ^{13}C n.m.r. characteristics of the C_α atoms.

In view of the relative electron richness of complex (1) {*cf.* $[Mo_2\{\mu\text{-}C_8(CO_2Me)_6H_2\}(\eta\text{-}C_5H_5)_2]$ with electron-withdrawing

† Since these values were not derived by an iterative self-consistent charge procedure, the magnitudes of the charges serve only to indicate the relative electron richness of the different parts of the molecule.

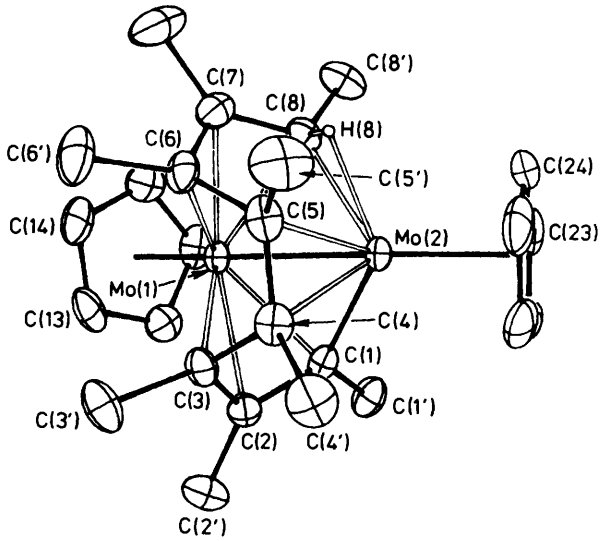

Figure 2. Molecular geometry of the cation $[Mo_2(\mu\text{-}C_8Me_8)(\mu_{Mo,C}\text{-}H)(\eta\text{-}C_5H_5)_2]^+$ present in complex (3)

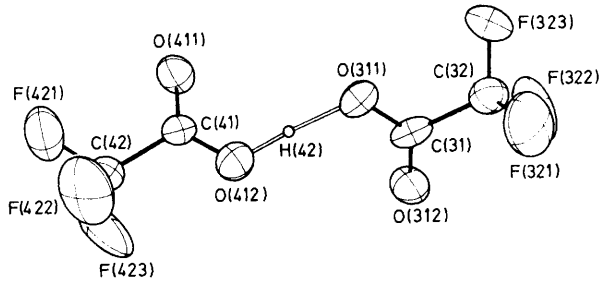

Figure 3. Molecular geometry of the anion $[(CF_3CO_2)_2H]^-$ present in complex (3)

substituents} its reactions with electrophiles, namely protonic acids, were studied. Treatment of complex (1) in diethyl ether with $HBF_4{\cdot}Et_2O$ or CF_3CO_2H gives quantitative yields of the purple crystalline complexes $[Mo_2(\mu\text{-}C_8Me_8)(\mu_{Mo,C}\text{-}H)(\eta\text{-}C_5H_5)_2][BF_4]$ (2) and $[Mo_2(\mu\text{-}C_8Me_8)(\mu_{Mo,C}\text{-}H)(\eta\text{-}C_5H_5)_2][(CF_3CO_2)_2H]$ (3) respectively. Similarly treatment of complex (1) with CF_3CO_2D gave the deuteriated analogue of complex (3), $[Mo_2(\mu\text{-}C_8Me_8)(\mu_{Mo,C}\text{-}D)(\eta\text{-}C_5H_5)_2][(CF_3CO_2)_2D]$ (4).

The ^1H n.m.r. spectra (see Table 1) of complexes (2) and (3) show the $Mo_2(\mu\text{-}C_8Me_8)(\eta\text{-}C_5H_5)_2$ core to be essentially intact, and that the C_s symmetry of complex (1) has been broken by protonation, *i.e.* eight CH_3 and two C_5H_5 resonances are observed. A high-field signal due to the proton derived from the acid is observed at δ −9.33 p.p.m., which shows coupling to two methyl groups. In order to define the site of protonation and the geometrical changes that result, an *X*-ray structure analysis of complex (3) was carried out.

The derived bond lengths and interbond angles within the cation and anion of complex (3) are given in Tables 4 and 5. The molecular geometry of the cation is shown in Figure 2, and that of the anion in Figure 3. The crystal structure of complex (3) consists of discrete molecular cations and complex hydrogen-bonded anions separated from one another by normal van der Waals distances.

The non-hydrogen-atom geometry of the cation of complex (3) is broadly similar to that of (1) showing no changes in connectivity nor major conformational rearrangement. The most interesting feature is the attachment of a hydrogen atom to both C(8) and Mo(2) [C(8)–H(8) 0.89(8) and Mo(2)–H(8) 1.88(8) Å] (see Figure 4, form Y).

Although the geometric parameters involving the bridging hydrogen atom are of necessity poorly determined by *X*-ray diffraction results, several features of the C–H–Mo system are clearly defined. The C–H–Mo linkage is markedly bent [C(8)–H(8)–Mo(2) 99(5)°] and there is considerable direct C(8)–Mo(2) interaction [C(8)–Mo(2) 2.196(5) Å] for which such bending is a precondition. The C(8)–Mo(2) distance shows the most marked bond-length difference between the cations of complexes (3) and (1) [Mo(2)–C_α in (1) is 2.092(2) Å]. This extension [by 0.104(6) Å] on protonation of a carbon–metal bond parallels similar lengthening of metal–metal bonds on protonation.[21] Taken with the geometric features above this may indicate broad similarities between C–H–M and M–H–M three-centre two-electron systems.

The other changes in geometry on protonation are minor indicating the rigidity of the central Mo_2C_8 framework. Substantial localization of the positive change on Mo(2) is indicated by the lengthening of the C(1)–Mo(2), C(5)–Mo(2), and C(4)–Mo(2) bonds relative to those in complex (1) [by 0.038(5), 0.053(5), and 0.007(5) Å respectively]. The Mo≡Mo distance in complex (3) is also slightly lengthened [by 0.019(2) Å]. Angular deformations in the C_8 chain are small, the intra-chain torsion angles being −37.7(5), 121.8(4), −2.5(5), −115.5(4), and 34.1(5)° [from C(1) to C(8)] with a maximum change of *ca.* 4° from values for complex (1). The changes in bond angles for C(8) are also small (<2.5°); of those at other chain carbon atoms that for Mo(2)–C(5)–C(5′) is the largest {increasing by 5.3(5)° to accommodate the steric requirements of H(8) [C(5) · · · H(8) 2.23(8) Å]}.

The anion of complex (3) consists of two CF_3CO_2 moieties linked by a short strong hydrogen bond, O(412) · · · O(311) 2.429(8) Å [*cf.* O · · · O 2.437(4) Å in $K(CF_3CO_2)_2H$ [22]]. As determined by *X*-ray diffraction the O–H–O system is marginally asymmetric, but essentially linear [O(311)–H(42) 1.35(7) and O(412)–H(42) 1.08(7) Å; O(311)–H(42)–O(412) 175(7)°]. The hydrogen-bonded oxygen atoms show longer C–O distances than those not so bonded [average 1.233(7) *vs.* 1.200(7) Å].

Thus, as shown in Scheme 1, protonation of complex (1) probably involves initial electrophilic attack at C_α followed by collapse of the unsaturated intermediate in a manner reminiscent of the initial stages of an α-hydrogen elimination reaction [23,24] to form the cation (2).

Insight into the solution-state structure of the cation $[Mo_2(\mu\text{-}C_8Me_8)(\mu_{Mo,C}\text{-}H)(\eta\text{-}C_5H_5)_2]^+$ was obtained by observation of the ^{13}C n.m.r. spectra of complexes (2) and (4) [the dideuteriated analogue of (3)] at temperatures between 192 and 295 K (see Experimental section). These spectra show resonances due to the two cyclopentadienyl groups, eight methyl-carbon resonances, and eight resonances, A, B, C, D, E (sum of two), F, and G [from low to high field; except at 233—295 K for (2) and 295 K for (4) where F > E] due to the eight carbon atoms of the C_8 chain. In general at 295 K the chemical shifts of these carbon atoms are at lower field than those of the corresponding atoms in complex (1), with the exception of two resonances at 144.5 and 64.4 p.p.m. (B and G), an expected trend in view of the positive charge. The two carbon resonances shifted upfield show significant proton couplings in the proton-coupled spectrum at 295 K: 48 and 24 Hz for the resonances at 144.5 and 64.4 p.p.m. respectively. *Both* these couplings are to the μ-H resonances to high field of $SiMe_4$, as demonstrated by selective decoupling of this proton. At lower temperatures these two ^{13}C resonances broaden markedly, therefore preventing observation of resolved coupling to the bridging proton. At 192 K the signal due to the

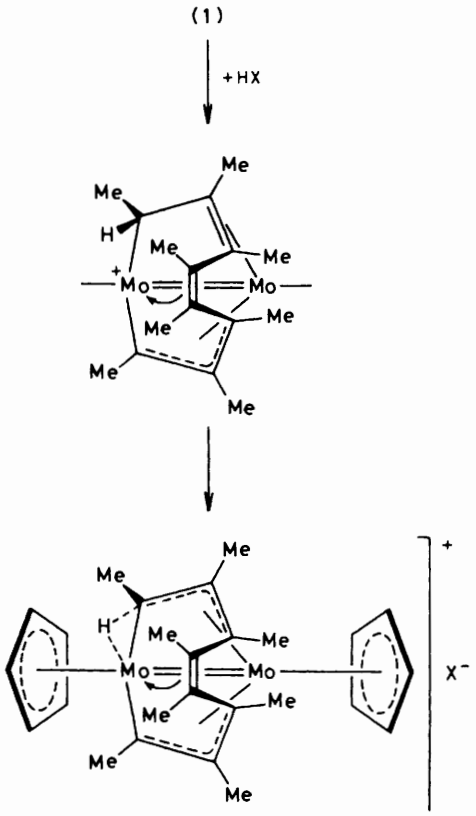

(2) $X^- = BF_4^-$
(3) $X^- = (CF_3CO_2)_2H^-$

Scheme 1.

lower-field resonances collapsed completely. The values of the chemical shifts for resonances B and G showed marked temperature dependence (see Table 7), the resonances separating with decrease in temperature. The cyclopentadienyl resonances showed little temperature dependence, and the remaining ring-carbon resonances showed slight variations with temperature, this being most marked for resonance F, which likewise showed marked broadening at low temperatures.

A reasonable interpretation of these observations is that the cation in solution undergoes a rearrangement, which is fast on the n.m.r. time-scale at room temperature. This rearrangement involves a site exchange of the bridging proton, such that it spends some time attached to the terminal atom of the C_8 chain, C_α, and the remainder of the time attached to one of the olefinic carbon atoms, C_δ, in *both* cases bridging from these to the molybdenum atom. Thus, in solution the cation $[Mo_2(\mu\text{-}C_8Me_8)(\mu_{Mo,C}\text{-}H)(\eta\text{-}C_5H_5)_2]^+$ is in equilibrium between the forms X and Y depicted in Figure 4. The observed chemical shifts for the chain carbon atoms are then averaged according to the relative proportions of forms X and Y present at any given temperature. The resonances B and G are assigned to C_α and C_δ respectively, and are those most effected by the equilibrium X ⇌ Y. By comparison with the ^{13}C spectrum of complex (1) resonance A may be assigned to $C_{\alpha'}$, C and D to C_β and $C_{\beta'}$, F to one of C_γ, $C_{\gamma'}$, or $C_{\delta'}$, and E to a superposition of the other two.

A quantitative analysis of the temperature dependence of resonances B and G is possible. In numerical terms, δ, the chemical shift of a given resonance is given by equation (i) where $K = [X]/[Y]$, the equilibrium constant between forms

Table 6. Analysis of $^{13}C\text{-}\{^1H\}$ n.m.r. data for complexes (2), (4), and (5) [a]

	(2)	(4)	(5) [b]
ΔH/kJ mol^{-1}	−2.6(4)	2.5(5)	−1.7(4)
ΔS/J K^{-1} mol^{-1}	−16.5(30)	−15.8(42)	−9.3(40)
B_X	191.0 [c]	191.0 [c]	191.0 [c]
B_Y	125(6)	126(8)	141(9)
G_X	27(9)	26(12)	35(10)
G_Y	80.0 [c]	80.0 [c]	80.0 [c]

[a] B_X and B_Y (G_X and G_Y) are chemical shifts (in p.p.m.) for the carbon atom giving rise to resonances B (G) in forms X and Y respectively; estimated standard deviations in the final digit are given in parentheses. [b] Labelling of C_δ resonances (H) in complex (5) is different from that in (2) (G) in Tables 7 and 8. [c] Parameters fixed at these values.

$$\delta = \frac{K}{1+K}\cdot\delta_x + \frac{1}{1+K}\cdot\delta_y \qquad \text{(i)}$$

X and Y, and δ_x and δ_y are the chemical shifts of the carbon atom in question in forms X and Y. If we assume that these chemical shifts, and likewise ΔH and ΔS for the reaction, are themselves not temperature dependent then in principle all these parameters may be evaluated from the n.m.r. data to hand. In practice this is feasible only for resonances B and G, which show the largest temperature variations. Unfortunately correlation between the six parameters to be determined (ΔH, ΔS, and four chemical shifts) precludes a full analysis given the limited temperature range for which experimental data are available. It is possible, however, to carry out a restricted analysis by fixing the values of certain of these parameters. The values of the chemical shifts of C_α and C_δ in forms X and Y respectively, *i.e.* B_X and G_Y in the notation of Table 6, were therefore fixed at values derived from the shifts of resonances A, E, and F. Least-squares analysis of the chemical shifts of resonances B and G at nine temperatures for complex (2) and three temperatures for complex (4) gave the values listed in Table 6. These values give root-mean-square (r.m.s.) discrepancies between observed and calculated chemical shifts for resonances B and G of 0.3 and 0.5 p.p.m. for complexes (2) and (4) respectively. The high estimated standard deviations in the derived parameters reflect the high correlation between parameters and the relatively small temperature range accessible. The apparent coupling constant between the bridging proton and carbon atoms C_α and C_δ at any given temperature may be calculated according to equation (ii), where J_X is the coupling constant in form X and J_Y that

$$J = \frac{K}{1+K}\cdot J_x + \frac{1}{1+K}\cdot J_Y \qquad \text{(ii)}$$

in form Y. To a good approximation we expect $J_X = 0$ for B and $J_Y = 0$ for G, in view of the unresolved couplings between the bridging proton and any chain carbon atoms other than C_α and C_δ. On this basis J_Y for B and J_X for G may be calculated from the observed couplings J at 295 K (48 and 24 Hz respectively) given the thermodynamic data of Table 6. These data give a value for K of 0.39 at 295 K, and thus values for the one-bond C–H coupling constants of J_Y (for B) = 66 Hz and J_X (for G) = 84 Hz. These values are typical (see refs. 2 and 23 and references therein) for such bridged C–H–M interactions, and as such indicate that the equilibrium constant at 295 K derived in this analysis is reasonable.

Although the above analysis is somewhat restricted by the assumptions made, several interesting features emerge.

Table 7. Variation in ^{13}C n.m.r. chemical shift (p.p.m.) with temperature for $[Mo_2(\mu\text{-}C_8Me_8)(\mu_{Mo,C}\text{-}H)(\eta\text{-}C_5H_5)_2][BF_4]$ (2) and $[Mo_2(\mu\text{-}C_8Me_8)(\mu_{Mo,C}\text{-}D)(\eta\text{-}C_5H_5)_2][(CF_3CO_2)_2D]$ (4)

								C_5H_5	
T/K	A	B	C	D	E	F	G		
Complex (2)									
192	191.22	—	127.92	120.37	80.91	79.78	—	99.52	97.07
203	191.51	151.40	127.92	120.56	81.03	80.77	59.0	99.45	97.11
213	191.69	150.26	127.92	120.70	81.14	80.92	59.9	99.45	97.14
223	191.91	148.54	127.99	120.85	81.21	81.21	61.20	99.45	97.22
233	192.06	147.70	128.03	120.99	81.28	82.05	61.98	99.45	97.25
243	192.17	146.89	128.10	121.10	81.39	82.39	62.50	99.45	97.29
251	192.31	146.20	128.17	121.21	81.55	82.53	63.11	99.49	97.33
260	192.39	145.87	128.21	121.25	81.58	82.79	63.40	99.49	97.37
273	192.46	145.28	128.28	121.40	81.65	83.08	63.96	99.56	97.40
295	192.51	144.48	128.22	121.45	81.61	83.08	64.35	99.54	97.43
Complex (4)									
208	191.53	152.50	128.08	120.53	81.10	80.7	58.44	99.51	97.12
243	192.17	148.10	128.27	121.00	81.53	81.0	61.90	99.51	97.29
295	192.65	146.00	128.66	121.45	82.00	83.0	63.65	99.64	97.50

Table 8. Variation in ^{13}C n.m.r. chemical shift (p.p.m.) with temperature for $[Mo_2(\mu\text{-}C_8Me_6Et_2)(\mu_{Mo,C}\text{-}H)(\eta\text{-}C_5H_5)_2][BF_4]$ (5)

									C_5H_5	
T/K	A	B	C	D	E	F	G	H		
178	190.08	—	128.65	121.40	86.78	78.54	74.70	—	99.34	97.18
193	190.20	165.32	128.76	121.54	86.96	78.61	75.06	57.84	99.34	97.22
203	190.34	164.89	128.88	121.66	87.08	78.65	75.21	58.25	99.39	97.30
213	190.45	163.96	128.91	121.73	87.25	78.76	75.50	58.94	99.42	97.33
233	190.48	162.77	128.80	121.73	87.29	78.76	75.83	59.67	99.25	97.20
251	190.85	162.13	129.20	122.10	87.73	79.09	76.45	70.64	99.52	97.51
263	191.00	161.58	129.27	122.20	87.88	79.20	76.14	61.21	99.56	97.59
295	191.14	160.78	129.42	122.39	88.10	79.34	77.04	61.80	99.60	97.66

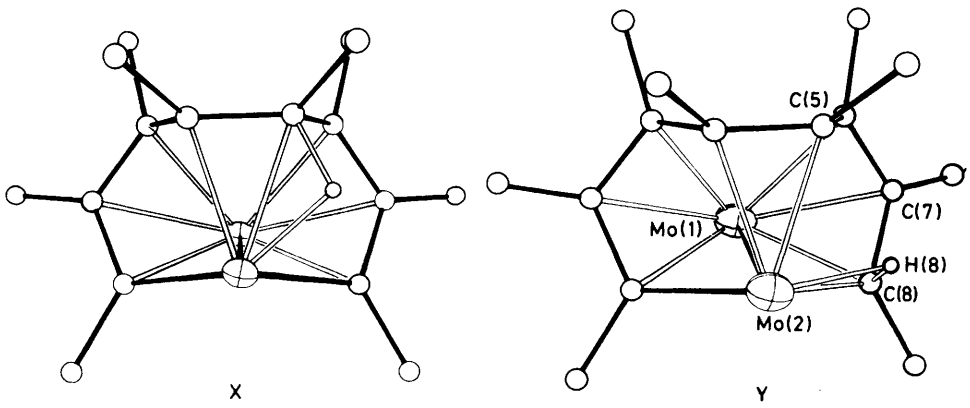

Figure 4. Geometries of isomeric forms X and Y; X is obtained from the structure of complex (3) by transfer of μ-H from C_α to C_δ Y is the cation of (3)

First, although form X has a lower heat content (ΔH being negative), Y is the dominant isomer in solution at all the temperatures at which spectra were measured. For complex (2), *K* varies between 0.398 at 295 K and 0.642 at 203 K, and Y is the isomer present in the solid-state structure of complex (3). Remarkably it is the entropy term in the free-energy difference between X and Y which dominates the temperature dependence of the equilibrium illustrated in Scheme 2. The spectra of complex (4), the deuteriated analogue of (3), indicate that there is a small effect that results in higher values of *K* over the temperature range observed [*K* for complex (4) varies between 0.430 at 295 K and 0.693 at 208 K]. This may be due either to an isotope effect or to the effect of the counter-anion in complex (3).

In order to provide further experimental evidence on the nature of the transannular hydrogen site-exchange process occurring in solution in complexes (2) and (3) we also studied the n.m.r. properties of $[Mo_2(\mu\text{-}C_8Me_6Et_2)(\mu_{Mo,C}\text{-}H)(\eta\text{-}C_5H_5)_2][BF_4]$, complex (5) (see Scheme 2 and Table 8). This species is derived from complex (1) by an extension of our published [25] method for modifying the substituents at a δ carbon atom of the μ-C_8 chain present in complex (1). Pro-

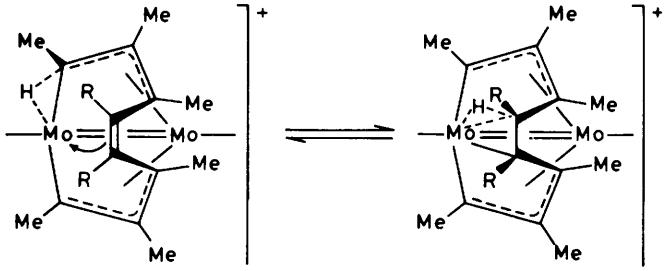

Form Y, R = Me (2) Form X, R = Me
Form Y, R = Et (5) Form X, R = Et

Scheme 2. η-C_5H_5 ligands omitted for clarity

tonation of the diethyl derivative of complex (1) with $HBF_4 \cdot Et_2O$ gave complex (5), characterized by elemental analysis and n.m.r. spectroscopy (see Table 1). As expected the major difference in the ^{13}C n.m.r. spectrum of complex (5) compared with that of (2) is in the positions of resonances designated B and G for complex (2). Thus, the chemical shifts of these resonances for complex (5) [(2) in square brackets] at 295 K are δ 160.8 [144.5] and 61.8 [64.4] p.p.m. for C_α and C_δ respectively. In addition the apparent $^1J_{CH}$ coupling constants observed for these resonances show substantial variations {29.4 [48] and 37 [24] Hz for C_α and C_δ for (5) [(2)]}. Thus complex (5) shows, as did (2), a rapid equilibrium between isomeric forms X and Y (Scheme 2), albeit with a different balance of isomers. A quantitative analysis of the temperature dependence of the chemical shifts of resonances **B** and H in complex (5) was also carried out, as for complexes (2) and (4), affording the parameters listed in Table 6. The r.m.s. difference between the observed and calculated chemical shifts is 0.14 p.p.m. These show equilibrium constants, K (=[X]/[Y], as before), ranging from 0.66 at 295 K to 0.95 at 193 K, consistently larger than those for complexes (2) and (4). Using these values of K the proton-coupled spectra at 295 K and 233 K give $^1J_{CH}$ values for the α carbon in form Y of 50 and 51 Hz respectively, and values for the δ carbon in X of 85 and 91 Hz.

It is tempting to ascribe the increased concentrations of form X present in solutions of complex (5), as compared to those of (2), to the inductive effect of the ethyl group stabilizing this isomer. Indeed EHMO calculations (discussed below) show a marked positive shift in the net charge on the carbon atom bridged; thus for C_δ the net charge in form Y is −0.22 e, and in form X 0.11 e, the corresponding figures for C_α being −0.19 and −0.56 e. However, quantitative analysis of the n.m.r. data indicates the change in equilibrium position to be associated primarily with the entropy contribution to the free-energy difference between forms X and Y in complex (5) as compared with (2). The enthalpy term for complex (5) shows a closer balance between X and Y, rather than an increased favourability for X as the above argument would indicate. We would hesitate to place too much confidence in the detail of the quantitative analysis particularly in this respect since the ΔH and ΔS terms are highly correlated.

The ^1H n.m.r. spectrum of complex (5) shows the bridging proton to be coupled to each of the diastereotopic protons of the methylene group on C_δ, and additionally to the methyl group on C_α as well as one of the methylene protons of the group on $C_{\delta'}$, with coupling constants ^4J(HH) of 1.7 and 2.8, and ^3J(HH) 1.5 and 1.6 Hz respectively. The high-field chemical shift of the bridging hydrogen (δ −9.72 p.p.m.) shows a change, relative to that in complex (2), in the same direction

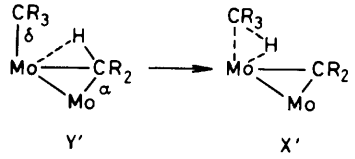

Y′ X′

Figure 5.

as does the dideuteriated cation (4). The large difference between the proton and deuterium chemical shifts for the bridging hydrogen may be a consequence either of the difference in chemical shifts of the two sites (attached to C_α or C_δ) or of the abnormally large isotope effects in these shifts. Such abnormally large isotope effects have been noted [26] for hydrogen atoms in highly asymmetric environments, *e.g.* in strongly hydrogen-bonded systems.

The rapid exchange between forms X and Y of the cation (2) is slowed sufficiently at 192 K for the signal B in the ^{13}C spectrum to collapse almost completely. This indicates an upper limit for the activation energy of this process of *ca.* 32 kJ mol^{-1}. The corresponding signal in the spectrum of complex (5) collapses at 178 K giving an upper limit of the activation energy of *ca.* 30 kJ mol^{-1}. Since the process involves metal-mediated cleavage of the C–H bonds involved, these bonds are clearly substantially activated by their interaction with the molybdenum atom. The passage of the hydrogen atom from C_α to C_δ is an intramolecular α-abstraction process. This process involves conversion as illustrated (Figure 5) of a CR_2H moiety (as in Y′) into a CR_2 moiety *via* metal-mediated transfer of the α-hydrogen to an adjacent CR_3 moiety (as in X′). Here the CR_2 group is bonded additionally to a second metal atom. The rigidity of the carbon-chain skeleton prevents full scission of the CR_3H-to-metal linkage formed in X′; indeed this C–H–Mo interaction is clearly a strong one. The Y′ ⟶ X′ reaction therefore models the central part of an α-abstraction reaction formally related to those observed [23] in mononuclear chemistry {*e.g.* '$Ta(CH_2CMe_3)_5$' ⟶ $[Ta(CH_2CMe_3)_3(CHCMe_3)] + CMe_4$}, there being no elimination of alkane here. Reaction X′ ⟶ Y′ models the reverse process, insertion of a metal into an alkane C–H bond, with transfer of the hydrogen atom to a co-ordinated carbene ligand, a reaction without precedent.

In order to probe further the nature of the cation present in complex (2), particularly with regard to the bridging hydrogen moiety, EHMO calculations were carried out on $[Mo_2(\mu\text{-}C_8H_8)(\mu_{Mo,C}\text{-}H)(\eta\text{-}C_5H_5)_2]^+$, using a molecular geometry based on that of complex (3) in the solid state. Variation of the position of the bridging hydrogen with the remaining atoms fixed confirmed that bridging (CHMo) sites were favoured over terminal CH or MoH sites on electronic grounds as reflected in the total energy of the molecular ion. The two forms of complex (2) observed in solution, *i.e.* X and Y, were found to have similar energies with form X favoured by *ca.* 0.1 eV, with C–H 1.25 and Mo–H 1.75 Å in both cases. Movement of the bridging hydrogen along the least-motion path between the two sites whilst holding MoH fixed at 1.75 Å gave a substantial barrier of *ca.* 1.1 eV to the interconversion of forms X and Y. Since no allowance is made in the calculations for geometric changes in the remainder of the molecule this energy difference cannot be accurate. These changes are likely to be fairly small in view of the similarity of the frameworks of complexes (1) and (3). We therefore conclude that the energy barrier calculated is likely to be an overestimate, as is indicated by the experimental data. The least-motion path, between the bridging sites for the proton which give reasonable bond angles at the carbon atoms, is short (*ca.* 1.4 Å), a factor

which may be important in determining the magnitude of the activation energy of the site-exchange process. However, in view of the fairly large discrepancy between the observed and EHMO-estimated activation energies (the latter assuming a near-least-motion pathway) alternative pathways cannot be excluded.

Experimental

All synthetic manipulations were carried out under a nitrogen atmosphere with use of conventional Schlenk techniques. All solvents were dried and distilled from sodium–benzophenone prior to use except CH_2Cl_2 which was distilled from phosphorus pentoxide. Deuteriated n.m.r. solvents were degassed prior to use. Proton and carbon-13 n.m.r. spectra were recorded on JEOL FX90Q and FX200 spectrometers, deuterium spectra on a JEOL FX200, and molybdenum-95 spectra on a Bruker WH400 spectrometer at 26.0 MHz. Proton and carbon-13 spectra were referenced internally to $SiMe_4$ (0.0 p.p.m., positive values to high frequency), deuterium spectra internally to $CDCl_3$, and molybdenum-95 spectra externally to Na_2MoO_4 (2 mol dm^{-3}) in NaOH. Mass spectra were recorded on an AEI MS-902 spectrometer operating at 70 eV.

The preparation of $[Mo(NCMe)(MeC_2Me)_2(\eta\text{-}C_5H_5)][BF_4]$ has been described previously.[27] The salt $Na[Fe(CO)_2(\eta\text{-}C_5H_5)]$ was prepared from $[Fe_2(CO)_4(\eta\text{-}C_5H_5)_2]$ by treatment of the dimer in tetrahydrofuran (thf) with sodium amalgam (12 h). The compounds $HBF_4{\cdot}Et_2O$, CF_3CO_2H, and CF_3CO_2D were obtained from Aldrich Chemical Co. and used without further purification.

Preparations.—$[Mo_2(\mu\text{-}C_8Me_8)(\eta\text{-}C_5H_5)_2]$, (1). A suspension of $[Mo(NCMe)(MeC_2Me)_2(\eta\text{-}C_5H_5)][BF_4]$ (2.0 g, 5.0 mmol) in thf (10 cm^3) was cooled to 0 °C. A solution of $Na[Fe(CO)_2(\eta\text{-}C_5H_5)]$ in thf was added, obtained from reduction with sodium amalgam of $[Fe_2(CO)_4(\eta\text{-}C_5H_5)_2]$ in thf [1 g (2.8 mmol) of dimer and 0.2 g of Na(excess)]. The mixture was allowed to warm to room temperature and stirred for 12 h after which the solvent was removed *in vacuo*. The dark residue was extracted with hexane–diethyl ether (90 : 10) affording a purple solution, which was chromatographed on alumina. Elution with hexane–diethyl ether (90 : 10) gave a purple band, which was collected and recrystallized (−30 °C) from pentane to give purple *crystals* of complex (1) (0.3 g, 22%) (Found: C, 58.4; H, 6.3%; *M*, 538. $C_{26}H_{34}Mo_2$ requires C, 58.0; H, 6.3%; *M*, 538). Further elution with diethyl ether gave $[Fe_2(CO)_4(\eta\text{-}C_5H_5)_2]$.

$[Mo_2(\mu\text{-}C_8Me_8)(\mu_{Mo,C}\text{-}H)(\eta\text{-}C_5H_5)_2][BF_4]$, (2). A slight excess of $HBF_4{\cdot}Et_2O$ was added dropwise with stirring to a cooled (0 °C) solution of complex (1) (0.2 g, 0.37 mmol) in diethyl ether (5 cm^3). The resultant purple precipitate was collected and washed twice with diethyl ether, and then recrystallized by slow diffusion of diethyl ether into a methylene chloride solution at −30 °C to give purple *crystals* of complex (2) (Found: C, 49.7; H, 5.5. $C_{26}H_{35}BF_4Mo_2$ requires C, 49.7; H, 5.5%). The analogous salt $[Mo_2(\mu\text{-}C_8Me_8)(\mu_{Mo,C}\text{-}H)(\eta\text{-}C_5H_5)_2][(CF_3CO_2)_2H]$ (3) (Found: C, 46.4; H, 4.5. $C_{30}H_{36}F_6Mo_2O_4$ requires C, 46.4; H, 4.5%) was prepared similarly, using CF_3CO_2H, and pentane rather than diethyl ether in recrystallization. Yields of complexes (2) and (3) were essentially quantitative. The n.m.r. spectral data for complex (2) are given in Table 1. The spectra of complex (3) are essentially identical to those of (2) with the exception that the ^1H spectrum is slightly broadened and has in addition a broad singlet signal at δ 13.5 p.p.m. [1 H, $(CF_3CO_2)_2H$].

Table 9. Crystal data and refinement details for complexes (1) and (3)

	(1)	(3)
Molecular formula	$C_{26}H_{34}Mo_2$	$C_{30}H_{36}F_6Mo_2O_4$
M	538.4	766.5
Space group	$P\bar{1}$ (by refinement)	$P2_1/c$
a/Å	8.449(1)	10.648(2)
b/Å	10.114(2)	15.119(4)
c/Å	14.872(3)	19.655(6)
α/°	86.66(2)	—
β/°	80.88(1)	105.30(2)
γ/°	63.78(1)	—
U/Å^3	1 125.6(4)	3 052.0(7)
Z	2	4
D_c/g cm^{-3}	1.587	1.666
λ/Å	0.710 69	0.710 69
μ(Mo-K_α)/cm^{-1}	11.0	8.4
2θ range/°	3—60	3—55
Indices inspected	$h, \pm k, \pm l$	$h, k, \pm l$
Data recorded	5 109	4 954
Unique data	4 774	4 114
Data used (N_o), $I \geqslant 3\sigma(I)$	4 635	3 781
Least-squares parameters (N_v)	319	411
R*	0.020	0.029
R'	0.025	0.034
S	1.72	1.28
g	0.000 06	0.000 23

* $R = \Sigma|F_o - |F_c||/\Sigma F_o$, $R' = [\Sigma w(F_o - |F_c|)^2/\Sigma wF_o^2]^{\frac{1}{2}}$, $S = [\Sigma w(F_o - |F_c|)^2/(N_o - N_v)]^{\frac{1}{2}}$, and $w = [\sigma^2(F_o^2)/4F_o^2 + gF_o^2]^{-1}$.

$[Mo_2(\mu\text{-}C_8Me_8)(\mu_{Mo,C}\text{-}D)(\eta\text{-}C_5H_5)_2][(CF_3CO_2)_2D]$ (4). This preparation proceeded as for complex (3), but with use of CF_3CO_2D. The ^1H and $^{13}C\text{-}\{^1H\}$ n.m.r. spectra are almost identical to those for (3); the ^1H signals at δ 13.5 and −9.33 p.p.m. disappeared and the two Me resonances coupled to the high-field proton resonance appeared as singlets. The D n.m.r. spectrum (CH_2Cl_2) showed signals at δ −9.64 (s, 1 D, C · · · D · · · Mo), 5.40 and 4.51 (each s, C_5H_4D natural abundance), and 13.98 p.p.m. [br s, $(CF_3CO_2)_2D$].

$[Mo_2(\mu\text{-}C_8Me_6Et_2)(\mu_{Mo,C}\text{-}H)(\eta\text{-}C_5H_5)_2][BF_4]$, (5). A solution of $[Mo_2(\mu\text{-}C_8Me_6Et_2)(\eta\text{-}C_5H_5)_2]$ [25] (0.5 g, 0.88 mmol) in diethyl ether (20 cm^3) was cooled to −78 °C. A slight excess of $HBF_4{\cdot}Et_2O$ was added dropwise and the stirred solution allowed to warm to room temperature. The resultant precipitate was washed with diethyl ether (3 × 20 cm^3), and then recrystallized by slow diffusion of diethyl ether into a methylene chloride solution at −30 °C affording purple *crystals* of complex (5) (Found: C, 50.7; H, 6.0. $C_{28}H_{39}BF_4Mo_2$ requires C, 51.4; H, 6.0%). N.m.r. data for complex (5) are given in Table 1.

X-Ray Diffraction Studies.—$[Mo_2(\mu\text{-}C_8Me_8)(\eta\text{-}C_5H_5)_2]$, (1). Large well shaped purple crystals of compound (1) were obtained from pentane solution at −30 °C. Crystal data are presented in Table 9. Intensity data were collected on a Nicolet P3m diffractometer at room temperature from a crystal ground to approximately spherical shape (diameter 0.37 ± 0.03 mm) mounted in a thin-walled glass capillary under dry nitrogen. Reflections were scanned in the θ–2θ mode, scan widths being 2.0° + $\Delta\alpha_1\alpha_2$, using graphite monochromated Mo-K_α radiation. Scan speeds were varied between 3.0 and 29.3° min^{-1} based on a 2-s pre-scan. If this pre-scan showed reflection intensity <40.0 counts s^{-1} it was not recorded. Background intensity was measured at the extremes of the scan range for a total time equal to half of the time spent

Table 10. Fractional atomic co-ordinates for complex (1) *

Atom	*x*	*y*	*z*	Atom	*x*	*y*	*z*
Mo(1)	0.318 78(2)	0.330 03(2)	0.233 32(1)	C(7′)	0.393 0(4)	0.244 3(4)	−0.000 2(2)
Mo(2)	0.441 98(2)	0.054 56(2)	0.278 30(1)	C(8′)	0.179 7(4)	0.119 7(3)	0.130 2(2)
C(1)	0.313 9(3)	0.230 2(3)	0.371 41(14)	C(11)	0.217 0(5)	0.589 7(3)	0.250 4(4)
C(2)	0.403 9(3)	0.318 3(3)	0.377 34(15)	C(12)	0.082 6(5)	0.553 6(3)	0.293 8(4)
C(3)	0.556 6(3)	0.282 7(3)	0.309 20(15)	C(13)	0.024 1(5)	0.500 4(3)	0.227 8(4)
C(4)	0.659 3(3)	0.120 8(3)	0.285 69(14)	C(14)	0.122 4(5)	0.503 7(3)	0.143 7(4)
C(5)	0.669 0(3)	0.080 1(3)	0.192 98(14)	C(15)	0.241 6(5)	0.558 9(3)	0.157 7(4)
C(6)	0.575 9(3)	0.204 9(3)	0.131 24(14)	C(11′)	0.062 1(14)	0.482 7(12)	0.163 2(8)
C(7)	0.433 1(3)	0.195 9(3)	0.095 39(14)	C(12′)	0.030 2(14)	0.516 6(12)	0.255 9(8)
C(8)	0.335 4(3)	0.138 2(3)	0.157 96 (14)	C(13′)	0.148 2(14)	0.571 6(12)	0.272 4(8)
C(1′)	0.149 1(4)	0.251 8(3)	0.439 7(2)	C(14′)	0.253 0(14)	0.571 7(12)	0.189 9(8)
C(2′)	0.345 5(5)	0.440 6(3)	0.447 9(2)	C(15′)	0.199 8(14)	0.516 8(12)	0.122 4(8)
C(3′)	0.662 0(4)	0.374 1(4)	0.301 1(3)	C(21)	0.577 5(5)	−0.207 6(3)	0.250 7(2)
C(4′)	0.809 3(4)	0.037 8(3)	0.342 3(2)	C(22)	0.623 6(4)	−0.187 7(3)	0.333 2(2)
C(5′)	0.828 3(3)	−0.052 4(3)	0.144 3(2)	C(23)	0.470 3(4)	−0.124 9(3)	0.397 3(2)
C(6′)	0.686 3(4)	0.274 9(4)	0.076 2(2)	C(24)	0.326 1(4)	−0.104 5(3)	0.354 2(3)
				C(25)	0.391 2(5)	−0.155 0(3)	0.264 1(3)

* C(11′)—C(15′) are the atoms of the disordered cyclopentadienyl groups of lower occupancy.

Table 11. Fractional atomic co-ordinates for complex (3)

Atom	*x*	*y*	*z*	Atom	*x*	*y*	*z*
Mo(1)	0.071 89(3)	0.152 93(2)	0.361 34(2)	C(25)	0.169 5(7)	0.331 9(5)	0.579 5(3)
Mo(2)	0.104 84(3)	0.233 37(2)	0.482 54(2)	C(11)	0.057 2(6)	0.002 2(3)	0.338 6(3)
C(1)	−0.070 5(5)	0.171 6(3)	0.424 5(3)	C(12)	−0.059 3(5)	0.039 0(4)	0.299 9(3)
C(2)	−0.132 9(4)	0.212 8(3)	0.359 0(3)	C(13)	−0.031 2(6)	0.094 2(4)	0.248 7(3)
C(3)	−0.056 0(4)	0.279 1(3)	0.339 1(2)	C(14)	0.102 0(6)	0.091 2(4)	0.255 9(3)
C(4)	0.022 3(5)	0.333 9(3)	0.398 9(3)	C(15)	0.157 2(5)	0.034 3(4)	0.311 5(3)
C(5)	0.160 0(5)	0.333 7(3)	0.408 3(3)	C(31)	−0.366 1(5)	0.207 4(4)	0.594 3(3)
C(6)	0.206 4(5)	0.274 2(3)	0.357 2(3)	C(32)	−0.369 5(6)	0.291 7(4)	0.552 8(4)
C(7)	0.285 9(5)	0.201 8(3)	0.387 1(3)	O(311)	−0.443 1(4)	0.208 3(3)	0.631 5(3)
C(8)	0.256 4(5)	0.162 3(3)	0.447 4(3)	O(312)	−0.288 4(5)	0.151 4(3)	0.589 1(3)
C(1′)	−0.139 1(5)	0.098 3(3)	0.454 1(3)	F(321)	−0.287 1(6)	0.350 0(3)	0.588 5(3)
C(2′)	−0.265 9(5)	0.188 3(4)	0.314 1(3)	F(322)	−0.329 0(7)	0.282 9(4)	0.496 2(3)
C(3′)	−0.102 7(6)	0.324 1(4)	0.267 7(3)	F(323)	−0.478 5(5)	0.329 4(4)	0.533 1(4)
C(4′)	−0.050 7(6)	0.415 1(3)	0.415 1(3)	C(41)	0.483 6(6)	0.450 4(4)	0.227 3(3)
C(5′)	0.241 6(6)	0.418 4(4)	0.428 9(4)	C(42)	0.516 4(7)	0.498 2(5)	0.297 2(4)
C(6′)	0.223 9(7)	0.317 5(4)	0.290 2(3)	O(411)	0.377 7(4)	0.457 6(3)	0.188 0(3)
C(7′)	0.394 7(6)	0.167 5(5)	0.357 4(4)	O(412)	0.576 4(5)	0.405 5(4)	0.221 0(3)
C(8′)	0.334 1(5)	0.085 1(4)	0.486 8(3)	F(421)	0.411 6(5)	0.532 9(4)	0.310 5(3)
C(21)	0.037 6(6)	0.316 8(4)	0.569 1(3)	F(422)	0.556 3(6)	0.448 0(4)	0.351 4(3)
C(22)	0.020 1(5)	0.228 0(4)	0.581 9(3)	F(423)	0.596 5(7)	0.559 4(5)	0.300 5(3)
C(23)	0.140 8(6)	0.187 3(4)	0.600 0(3)	H(8)	0.269(7)	0.216(5)	0.466(4)
C(24)	0.234 8(5)	0.252 4(6)	0.599 1(3)	H(42)	−0.427(7)	0.144(5)	0.680(4)

scanning the reflection. An empirical absorption correction, based on a six-parameter fit to 390 azimuthal scan data measured for seven independent reflections, was applied, giving transmission coefficients in the range 0.773—0.731 for the full data set. Lorentz and polarization corrections were applied.

The structure was solved by conventional heavy-atom methods. The molybdenum atoms were located by inspection of the Patterson function and all carbon atoms from a Fourier difference synthesis calculated after full-matrix blocked-cascade least-squares refinement of positional and thermal parameters for these atoms. The cyclopentadienyl group attached to Mo(1) showed two orientations with occupancy factors 0.773(8) and 0.227(8) respectively; both orientations were constrained to D_{5h} symmetry with a C–C bond length of 1.420 Å. The molybdenum and all carbon atoms, except those of the low-occupancy cyclopentadienyl group, were assigned anisotropic thermal parameters. After refinement of the non-hydrogen framework of the molecule all hydrogen atoms (except those of the low occupancy η-C_5H_5 ring) were located in a electron-density difference synthesis. All hydrogen atoms were then incorporated in the refined model with C–H bond lengths fixed at 0.96 Å and angular constraints (C–C–H angles 126.0° for the cyclopentadienyl hydrogen atoms and H–C–H angles 109.5° for methyl hydrogen atoms); their isotropic thermal parameters were allowed to refine freely. The weighting factor g (see Table 9 and footnote) was chosen to minimize the variation of $w|F_o - F_c|^2$ with the magnitude of F_o. Residual features on the final electron-density difference map were <0.33 e Å^{-3} in magnitude, the largest being <0.8 Å from the metal atoms and near the centre of C–C bonds. Details of the refinement results are given in Table 9 and derived atomic positional parameters are in Table 10.

All calculations used the SHELXTL program package in a Nicolet R3m/E structure-determination system. Complex neutral atom scattering factors taken from ref. 28 were used for all atoms.

$[Mo_2(\mu\text{-}C_8Me_8)(\mu_{Mo,C}\text{-}H)(\eta\text{-}C_5H_5)_2][(CF_3CO_2)_2H]$ (3). Small purple crystals of complex (3) were grown from pentane–methylene chloride solution at −30 °C. A crystal of dimensions *ca.* 0.20 × 0.15 × 0.12 mm, elongated along *a*, was

mounted under nitrogen in a thin-walled glass capillary for data collection. Crystal data are listed in Table 9. The data-collection technique and conditions were as for (1) with the exception that scan speeds varied between 0.8 and 29.3° min^{-1} and reflections with pre-scan intensities less than 12 counts s^{-1} were not recorded. No absorption correction was applied.

The structure analysis of complex (3) proceeded as for (1) without any disorder of the cyclopentadienyl ligands. All methyl and cyclopentadienyl hydrogen atoms were located on Fourier difference syntheses. The oxygen-bound hydrogen, H(42), and the ($\mu_{Mo,C}$-H) hydrogen, H(8), were located as the highest residual electron-density peaks of the anion and cation respectively after inclusion of the other hydrogen atoms as for complex (1). Atoms H(42) and H(8) were allowed to refine without constraint of either their positional or isotropic thermal parameters. Final atomic positional parameters for complex (3) are listed in Table 11. Details of computational procedures, *etc.* were as for complex (1).

Acknowledgements

We thank the S.E.R.C. for support and for studentships (to N. C. N. and C. J. S.) and Dr. B. E. Mann for ^{95}Mo n.m.r. results.

References

1 Part 30, S. R. Allen, S. G. Barnes, M. Green, G. Moran, L. Trollope, N. W. Murrall, A. J. Welch, and D. M. Sharaiha, *J. Chem. Soc., Dalton Trans.*, 1984, 1157.
2 M. Brookhart, W. Lamanna, and H. B. Humphrey, *J. Am. Chem. Soc.*, 1982, **104**, 2117, and references therein.
3 A. H. Janowicz and R. G. Bergmann, *J. Am. Chem. Soc.*, 1982, **104**, 352; J. K. Hoyano and W. A. G. Graham, *ibid.*, p. 3723.
4 R. H. Crabtree, J. M. Mihelcic, and J. M. Quirk, *J. Am. Chem. Soc.*, 1979, **101**, 7738; R. H. Crabtree, P. C. Demur, D. Eden, J. M. Mihelcic, C. A. Parnell, J. M. Quirk, and G. E. Morris, *ibid.*, 1982, **104**, 6994; D. Baudry, M. Ephritikine, and H. Felkin, *J. Chem. Soc., Chem. Commun.*, 1980, 1245.
5 M. Green, N. C. Norman, and A. G. Orpen, *J. Am. Chem. Soc.*, 1981, **103**, 1269.
6 S. A. R. Knox, R. F. D. Stansfield, F. G. A. Stone, M. J. Winter, and P. Woodward, *J. Chem. Soc., Dalton Trans.*, 1982, 173; S. R. Finnimore, S. A. R. Knox, and G. E. Taylor, *ibid.*, p. 1783.
7 A. M. Boileau, A. G. Orpen, R. F. D. Stansfield, and P. Woodward, *J. Chem. Soc., Dalton Trans.*, 1982, 187.
8 W. Geibel, G. Wilke, R. Goddard, C. Kruger, and R. Mynott, *J. Organomet. Chem.*, 1978, **160**, 131.
9 M. Green, N. C. Norman, A. G. Orpen, K. E. Paddick, and C. J. Schaverien, unpublished work.
10 A. F. Dyke, J. E. Guerchais, S. A. R. Knox, J. Roué, R. L. Short, G. F. Taylor, and P. Woodward, *J. Chem. Soc., Chem. Commun.*, 1981, 537.
11 A. F. Dyke, S. A. R. Knox, P. J. Naish, and G. E. Taylor, *J. Chem. Soc., Chem. Commun.*, 1980, 803.
12 G. K. Barker, W. E. Carroll, M. Green, and A. J. Welch, *J. Chem. Soc., Chem. Commun.*, 1980, 1071.
13 J. C. Jeffery, I. Moore, H. Razay, and F. G. A. Stone, *J. Chem. Soc., Chem. Commun.*, 1981, 1255.
14 J. A. Potenza, R. J. Johnson, R. Chivio, and A. Efraty, *Inorg. Chem.*, 1977, **16**, 2354.
15 I. B. Benzon, S. D. Killops, S. A. R. Knox, and A. J. Welch, *J. Chem. Soc., Chem. Commun.*, 1980, 1137.
16 M. H. Chisholm, R. L. Kelly, W. W. Reichert, F. A. Cotton, and M. W. Extine, *Inorg. Chem.*, 1978, **17**, 2944.
17 M. H. Chisholm, R. L. Kelly, F. A. Cotton, and M. W. Extine, *J. Am. Chem. Soc.*, 1978, **100**, 2256.
18 Program ICON8: J. Howell, A. Rossi, D. Wallace, K. Haraki, and R. Hoffmann, *Quantum Chemistry Program Exchange*, 1977, **10**, 344; R. H. Summerville and R. Hoffmann, *J. Am. Chem. Soc.*, 1979, **101**, 3821.
19 D. C. Calabro, D. L. Lichtenberger, and W. A. Herrmann, *J. Am. Chem. Soc.*, 1981, **103**, 6852.
20 D. A. Clementre, H. Cingi Biangini, B. Rees, and W. A. Herrmann, *Inorg. Chem.*, 1982, **21**, 3741.
21 R. G. Teller and R. Bau, *Struct. Bonding (Berlin)*, 1981, **44**, 1 and refs. therein.
22 A. L. MacDonald, J. C. Speakman, and D. Hadzi, *J. Chem. Soc., Perkin Trans. 2*, 1972, 825.
23 R. R. Schrock, *Acc. Chem. Res.*, 1979, **12**, 98.
24 R. J. Goddard, R. Hoffmann, and E. D. Jemmis, *J. Am. Chem. Soc.*, 1980, **102**, 7667.
25 S. G. Bott, N. G. Connelly, M. Green, N. C. Norman, A. G. Orpen, J. F. Paxton, and C. J. Schaverien, *J. Chem. Soc., Chem. Commun.*, 1983, 378.
26 L. J. Altman, D. Laungani, G. Gunnarsson, H. Wennerström, and S. Forsén, *J. Am. Chem. Soc.*, 1978, **100**, 8264.
27 S. R. Allen, P. K. Baker, S. G. Barnes, M. Green, L. Trollope, L. Manojlović-Muir, and K. W. Muir, *J. Chem. Soc., Dalton Trans.*, 1981, 873.
28 'International Tables for *X*-Ray Crystallography,' eds. J. A. Ibers and W. C. Hamilton, Kynoch Press, Birmingham, 1974, vol. 4, Table 2.2A.

Received 7th October 1983; *Paper* 3/1777